Micro-Doppler Removal in Radar Imaging in the Case of Non-Compensated Rigid Body Acceleration

Miloš Brajović, *Student Member*, *IEEE*, Ljubiša Stanković, *Fellow*, *IEEE*, Miloš Daković, *Member*, *IEEE*

***Abstract* — The micro-Doppler (m-D) effect, commonly caused by fast moving reflectors, can significantly decrease the readability of rigid body in ISAR/SAR radar images. We revisit an L-statistics based micro-Doppler removal approach, producing excellent results in separation of the stationary rigid body from the m-D. In the case of non-compensated target acceleration, rigid body components become non-stationary, commonly with linear frequency modulation. The Local Polynomial Fourier Transform (LPFT) can be exploited for the estimation of the unknown chirp-rate needed for the acceleration compensation. To this aim, we present a simple iterative procedure based on the LPFT concentration measure. It is an alternative to the direct search approach for the estimation of the LPFT demodulation parameter, improving the estimation accuracy and reducing the numerical complexity of the approach. Numerical examples verify the presented theory.**

***Keywords* —L-statistics, Local Polynomial Fourier Transform, L-statistics, ISAR/SAR, micro-Doppler, Short-time Fourier transform**

I. Introduction

Radar imaging is an important application field of the time-frequency signal analysis [1]- [11]. Micro-Doppler (m-D) effect usually appears in radar signals due to the presence of fast rotating or vibrating parts of the target [1]- [8]. Significant research efforts have been conducted towards the separation of the rigid body and m-D components in the received radar signals, in order to focus radar images and improve the readability [1]- [8]. Micro-Doppler signal parts are highly non-stationary, for rotating and vibrating targets commonly modeled with sinusoidally frequency modulated (FM) components, whereas the rigid body is stationary in the case of compensated target acceleration. Non-compensated movement of rigid body reflectors is commonly modeled with linear FM components in the received radar signal [1], [2].

Recently, a powerful and yet numerically efficient procedure for the separation of the rigid body from m-D has been proposed [1]. In the case of compensated movement it outperforms other reported techniques. It is based on the Short-time Fourier transform (STFT) and L-statistics. Further, it inspired new compressive sensing approaches for the rigid body reconstruction [11]. Moreover, the efficiency of the method was also confirmed in the case of rigid body with uncompensated acceleration, where the Local Polynomial Fourier Transform (LPFT) is proposed as the initial TF representation. However, the application of this representation requires the estimation of the chirp-rate parameter serving for the movement compensation, which is a priori unknown [1], [2]. Therefore, a direct search approach has been engaged to find the parameter value producing the optimal concentration measure of the separated rigid body [1], [12]. This value is impossible to find based on the original signal, and the L-statistics rigid body separation must be included in the search procedure. This process can be numerically demanding, especially for large search spaces and signals. In this paper we propose an automated and accurate gradient-based procedure for finding the optimal value of this parameter. It is also based on the time-frequency concentration measure.

In Section II, the basic background theory is presented. The STFT-based rigid body separation algorithm is presented in Section III. New search procedure for the acceleration compensation parameter is introduced in Section IV, and the subsequent section contains the numerical results.

Authors are with the Faculty of Electrical Engineering, University of Montenegro, Dzordza Vasingtona bb, 81000 Podgorica, Montenegro, e-mail: {milosb, ljubisa, milos}@ac.me

II. Background theory and the signal model

Consider a continuous wave (CW) radar transmitting signals in form of N coherent chirps. If $d(t)$ denotes the target distance, and c the speed of light, then the signal reflected from target is delayed for $t_d = 2d(t)/c$ with respect to the transmitted signal. Signal demodulation to the baseband, possible distance compensation and other standard preprocessing operations are assumed in the model [1].

The Doppler part of the received signal of a point target in the continuous dwell time will be considered only,

$$s(t) = \sigma e^{\frac{j2d(t)\omega_0}{c}}, \tag{1}$$

in order to analyze cross-range non-stationarities in the radar imaging, as it is commonly done in the radar literature [1], [2]. In (1), the target reflection coefficient is denoted by σ, and ω_0 is the radar operating frequency. It is assumed that the pulse repetition time is T_r with N_c samples within each chirp, and that the coherence integration time (CIT) is $T_c = NT_r$.

It is assumed that the Doppler part of the received signal corresponding to the rigid body can be modeled with complex sinusoids [1], [2]. In case of non-compensated target acceleration, the rigid body would induce linear FM components [1], [2]. Targets are usually consisted of fast moving vibrating and rotating parts, producing additional non-stationary components in the received signal - the micro-Doppler. Arbitrary m-D motion is modeled with an arbitrary FM signal. However, commonly appearing rotating or vibrating reflector produces the m-D modeled with sinusoidally FM signal. In the case of system of point scatterers, the received signal is modeled as a sum of individual scatterer responses. In the case of rigid body

consisted of K points and D m-D components the radar signal has the following form [1], [2]

$$s(n) = \sum_{i=1}^{K} \sigma_{B_i} e^{jy_{B_i} n} + \sum_{i=1}^{D} \sigma_{R_i} e^{jA_{R_i} \sin(\omega_{R_i} n + \Theta_i)}, \quad (2)$$

where $n = 0, ..., N-1$, and with σ_{B_i} and σ_{R_i} being reflection coefficients of the rigid body and rotating reflectors, y_{B_i} corresponds to the position of the rigid body reflector, A_{R_i} is proportional to the distance from the rotating reflector to the center of rotation. Angle frequencies ω_{R_i} are proportional to the rotating rate of the ith m-D reflector.

III. The Rigid Body Separation: Stationary Case

The method presented in [1] is independent from the assumed m-D model, and excellent results are obtained for arbitrary highly non-linear motion of m-D points. In further analysis, it is assumed that the received signal $s(t)$ is sampled according to the sampling theorem, and the discrete samples $s(n)$ are available for the analysis. Although the rigid body components are stationary, as m-D part has highly variable frequency content, the Fourier transform (FT) is not an adequate tool for the analysis of these signals, as it will be illustrated in numerical examples. Therefore, the time-frequency based approaches are exploited. Localization of the frequency behavior is achieved in the simplest way applying a window function to the standard FT. In this way, we obtain one form of the discrete short-time Fourier transform (STFT):

$$STFT(n,k) = \sum_{m=0}^{N-1} s(m) w(m-n) e^{-j2\pi mk/N}, \quad (3)$$

with $w(m)$ being the window function. In this application, rectangular, Hamming, Hanning and other standard window forms satisfying $\sum_{n=0}^{M-1} w(m-n) = const$ can be used. The window width is M, and $w(n) \neq 0$ for $-M/2 \leq w(m) \leq M/2 - 1$ and it is zero padded up to the signal length N. Therefore, original FT concentration can be obtained from (3) calculating

$$\begin{aligned} S(k) &\approx \sum_{n=M/2}^{N-M/2} STFT(n,k) \\ &= \sum_{m=0}^{N-1} s(m) \left[\sum_{n=M/2}^{N-M/2} w(m-n) \right] e^{-j2\pi mk/N}. \end{aligned} \quad (4)$$

As the resulting window $\sum_{m=M/2}^{N-M/2} w(n-m)$ is constant during the CIT interval, it is very close to a rectangular case (except for ending M/2 points at both sides). Therefore, (4) can be considered as the Fourier transform, with concentration close to the Fourier transform calculated with a full range rectangular window. The m-D can be removed from the $STFT(n,k)$ sorting its values over time, and removing a certain percent of highest values. Summing the remaining points over the frequency, a FT approximation of the rigid body is obtained. More precisely, the L-statistics based m-D removal can be done as follows:

Step 0: Calculate the STFT of the analyzed signal according to (3).

Step 1: Starting from a given set of STFT points

$$\mathbf{S}_k(n) = \{STFT(n,k),\ n = M/2, ..., N - M/2\} \quad (5)$$

sort the values of this set over the time index n to obtain a new, ordered set of elements, $\Lambda_k(n_i) \in \mathbf{S}_k(n)$, $n_i \in \{M/2, \ldots, N - M/2\}$ satisfying, for a given frequency index k:

$$|\Lambda_k(n_1)| \leq |\Lambda_k(n_2)| \leq \cdots \leq |\Lambda_k(n_{N-M})|. \quad (6)$$

It is important to note that holds

$$S_\lambda(k) = \sum_{n=M/2}^{N-M/2} STFT(n,k) = \sum_{i=1}^{N-M} \Lambda_k(n_i). \quad (7)$$

Step 2: Omit highest N_P values from $\mathbf{\Lambda}_k(n_i)$, with $N_P = \text{int}[(N-M)(1-P)/100]$ and P being the percent of omitted values.

Step 3: Based on the obtained subset L_k of $\{n_1, n_2, \ldots, n_{N-M}\}$, calculate the L-estimate

$$S_L(k) = \sum_{n \in L_k} STFT(n,k). \quad (8)$$

In this result, STFT values belonging to the rigid body peak will be summed in phase, producing a highly concentrated peak in the FT domain. The low concentrated m-D components remaining after the removal of $N - N_Q$ STFT points for each k will be summed up by different random phases. A more detailed discussion of this result is presented in [1] and [2].

IV. Non-compensated Rigid Body Acceleration

As noted in [1], in both ISAR and SAR received radar signals, accelerating target motion produces linear FM signals corresponding to the rigid body reflectors. Therefore, stationary components in (2) are replaced with linear FM components, having an unknown chirp-rate a. In this paper we consider the simplified case of parallel linear FM components. This means that the resulting rigid body becomes non-stationary, and the procedure presented in previous section would eliminate significant parts of the rigid body. An LPFT based dechirping technique can be exploited in this case. Namely, the LPFT of the following form

$$LPFT_\alpha(n,k) = \sum_{m=-M/2}^{M/2-1} s(n+m) w(m) e^{-j2\pi[\frac{m}{M}k + \alpha(\frac{m}{M})^2]},$$

can be used to determine the optimal chirp rate $\alpha_{opt} = a$. It is impossible to estimate the unknown dechirping parameter α using the original signal. Therefore, a similar procedure for separation of rigid body as presented in Section III is used in the following α estimation algorithm.

Step 0: Initialize $\nabla = \max[|(x(n)|]$ and $\alpha^{(0)} = 0$.

Then, repeat Steps 1-3 until a stopping criterion is met:

Step 1: Calculate:

$$\begin{aligned} &LPFT_{\alpha^+}(n,k) \\ &\quad = \sum_{m=-M/2}^{M/2-1} s(n+m) w(m) e^{-j2\pi[\frac{m}{M}k + (\alpha+\nabla)(\frac{m}{M})^2]}, \\ &LPFT_{\alpha^-}(n,k) \\ &\quad = \sum_{m=-M/2}^{M/2-1} s(n+m) w(m) e^{-j2\pi[\frac{m}{M}k + (\alpha-\nabla)(\frac{m}{M})^2]}, \end{aligned}$$

Step 2: Apply the L-statistics as described in Section III on both $LPFT_{\alpha^+}(n,k)$ and $LPFT_{\alpha^-}(n,k)$. Starting from given sets of LPFT points

$$\mathbf{L}_k^{\pm}(n) = \{LPFT_{\alpha^{\pm}}(n,k),\ n = M/2, ..., N - M/2\}$$

sort the values of these sets over n to obtain new, ordered sets of elements, $\Lambda_k^+(n_i) \in \mathbf{L}_k^+(n)$, and $\Lambda_k^-(n_j) \in \mathbf{L}_k^-(n)$, $n_i, n_j \in \{M/2, \ldots, N - M/2\}$ satisfying, for given k: $|\Lambda_k^+(n_1)| \leq |\Lambda_k^+(n_2)| \leq \cdots \leq |\Lambda_k^+(n_{N-M})|$ and $|\Lambda_k^-(n_1)| \leq |\Lambda_k^-(n_2)| \leq \cdots \leq |\Lambda_k^-(n_{N-M})|$.

Highest N_Q values from $\mathbf{\Lambda}_k^+(n_i)$ and N_Q values from $\mathbf{\Lambda}_k^-(n_j)$ are omitted, where $N_Q = \text{int}[(N - M)(1 - Q)/100]$ and Q is the percent of omitted values.

Based on the obtained subsets L_k^+ and L_k^- of $\{n_1, n_1, \ldots, n_{N-M}\}$, calculate

$$S_L^+(k) = \sum_{n \in L_k} LPFT_{\alpha^+}(n,k), \tag{9}$$

$$S_L^-(k) = \sum_{n \in L_k} LPFT_{\alpha^-}(n,k). \tag{10}$$

Step 2: Approximate the concentration measure [12] gradient as the difference of the form:

$$\nabla = \sum_{k=0}^{M-1} |S_L^+(k)| - \sum_{k=0}^{M-1} |S_L^-(k)|. \tag{11}$$

The idea to approximate the gradient in this way was presented in several recent papers, for example, in [13].

Step 3: Update the parameter in the gradient direction:

$$\alpha^{(l+1)} = \alpha^{(l)} - \mu\nabla. \tag{12}$$

The resulting parameter α is further used to demodulate the signal and apply the m-D removal and rigid body reconstruction algorithm presented in Section III. In numerical examples, step $\mu = \frac{M}{N_Q}$ is used. The iteration index is denoted by l. Detailed analysis of the optimal step value is part of our further research.

V. Numerical results

In numerical examples, signal of the form

$$s(n) = \sum_{i=1}^{K} \sigma_{B_i} e^{j2\pi[a(\frac{n}{N})^2 + b_i \frac{n}{N}]}$$
$$+ \sum_{i=1}^{D} \sigma_{R_i} e^{jA_{R_i} \sin(\omega_{R_i} n + \Theta_i) + j2\pi c_i \frac{n}{N} + j2\pi d_i (\frac{n}{N})^2} + \epsilon(n)$$

will be observed. It can be considered that such signal corresponds to a range bin in a radar image. First summation simulates rigid body reflectors with non-compensated acceleration a. The second term simulates m-D, whereas $\epsilon(n)$ is additive, zero-mean, white complex noise with i.i.d. real and imaginary parts, having the Gaussian distribution and the resulting variance σ_ϵ^2. Signal length is $N = 1024$ and Hanning window of length $M = 128$ is used.

Example 1: In this example, $K = 5$ rigid body components exist, with $\sigma_{B_i} = [0.5, 0.25, 0.25, 1, 1]$, $b_i = [160, 40, 60, 290, 310]$ for $i = 1, ..., 5$, respectively. The unknown chirp rate is $a = 360$. Only one m-D component is present, meaning that $D = 1$. Other parameters are: $\sigma_{R_1} = 4$, $\Theta_1 = 0$, $A_{R_1} = 120$, $\omega_{R_1} = 2$, $c_1 = 20$ and $d_1 = 0$. Signal is noiseless in this example. It is processed using presented approaches, and results are presented in Fig. 1. The initial signal STFT is shown in Fig. 1a, and the corresponding FT is presented in Fig. 1c. The STFT-based rigid body and m-D separation does not produce satisfactory results, as significant rigid body parts are removed. Namely, sorted STFT values are shown in Fig. 1b, whereas the rigid body after the m-D removal is shown

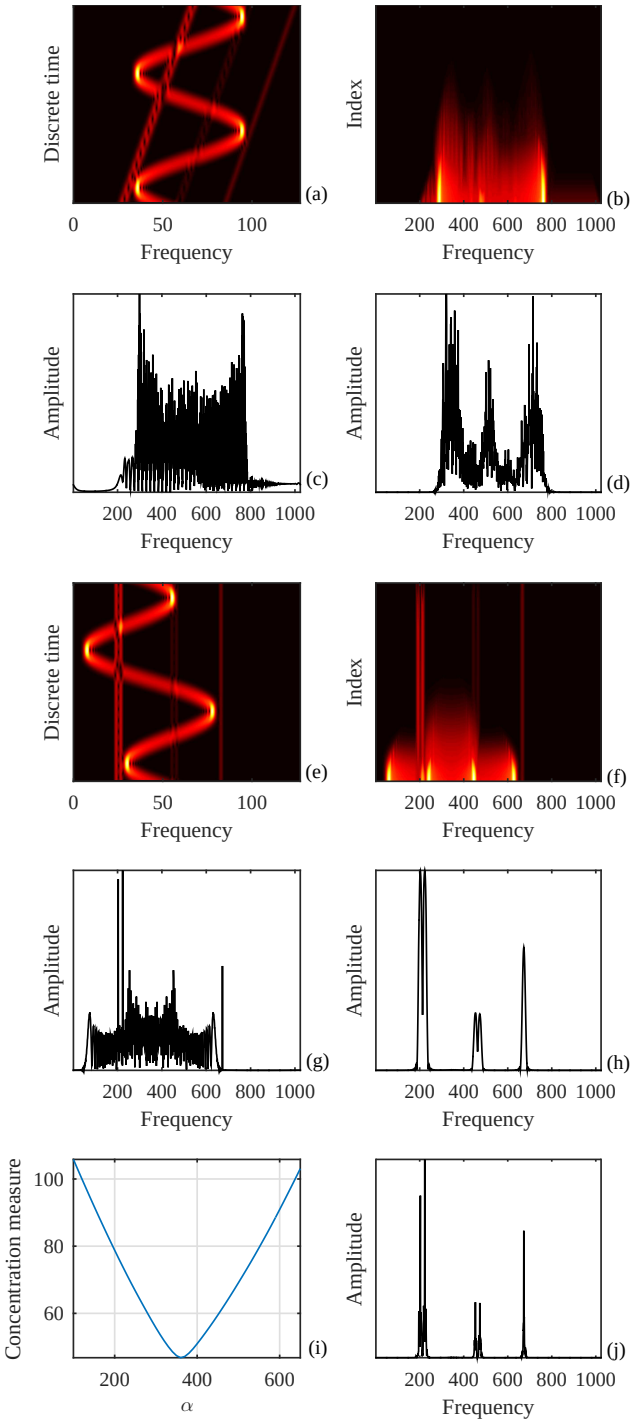

Fig. 1. Rigid body and m-D separation in the case of uncompensated rigid body acceleration. (a) The STFT of the original signal. (b) Sorted STFT values. (c) FT of the original signal. (d) FT obtained summing lowest 40% of the STFT over time. (e) STFT of the signal dechirped with optimal α. (f) Sorted dechirped signal STFT values. (g) FT of the dechirped signal. (h) FT obtained summing lowest 40% of absolute values of the dechirped signal STFT over time. (i) Concentration measure used for chirp-rate α optimization shown as function of α. (j) FT obtained summing lowest 40% of the dechirped signal STFT over time, using (8).

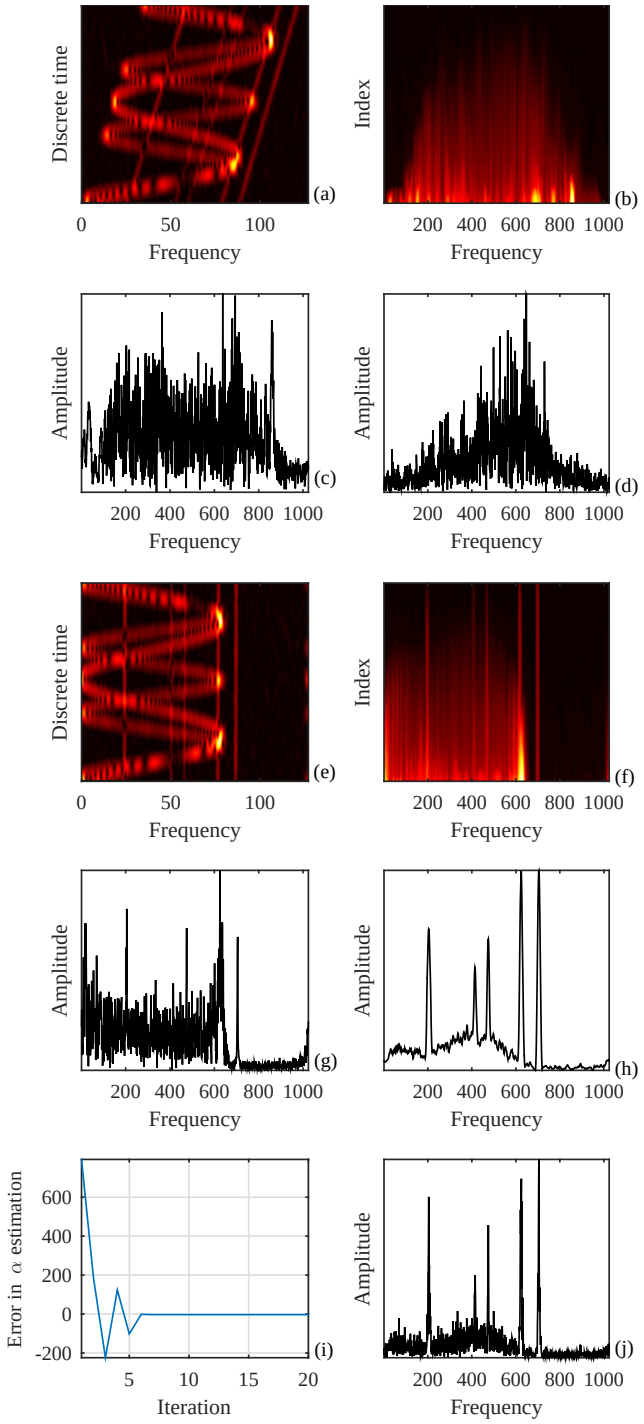

Fig. 2. Rigid body and m-D separation in the case of uncompensated rigid body acceleration - noisy signal case. (a) The STFT of the original signal. (b) Sorted STFT values. (c) FT of the original signal. (d) FT obtained summing lowest 40% of the STFT over time. (e) STFT of the signal dechirped with optimal α. (f) Sorted dechirped signal STFT values. (g) FT of the dechirped signal. (h) FT obtained summing lowest 40% of absolute values of the dechirped signal STFT over time. (i) Parameter α during the optimization algorithm iterations. (j) FT obtained summing lowest 40% of the dechirped signal STFT over time according to (8).

in Fig. 1d. Optimal chirp rate $\alpha = 360$ was found using the proposed approach. STFT of the signal dechirped with this value is shown in Fig. 1e, whereas the corresponding FT is shown in Fig. 1g. Sorted STFT values of the dechirped signal are presented in Fig. 1f, and the FT reconstructed summing $P = 40\%$ the lowest absolute values is shown in Fig. 1h. FT reconstructed summing sorted STFT values according to (8) is shown in Fig. 1j. Concentration measure used in chirp rate estimation algorithm, Step 2, defined as $\mathcal{M}_\alpha = \sum_{k=0}^{M-1} |S_L(k)|$ obtained varying α in range $[100, 600]$ with step 1 is shown in Fig. 1d.

Example 2: Considered signal has $K = 5$ rigid body components, with $\sigma_{B_i} = [1, 0.5, 0.5, 1, 1]$, $b_i = [190, 40, 100, 310, 110]$ for $i = 1, ..., 5$, respectively. The unknown chirp rate is $a = 300$. There are two m-D components, $D = 2$. Other parameters are: $\sigma_{R_1} = 4$, $\sigma_{R_2} = 4$, $\Theta_1 = N/2$, $\Theta_2 = \pi/2$, $A_{R_1} = 160$, $A_{R_2} = 90$, $\omega_{R_1} = 4$, $\omega_{R_2} = 7$, $c_1 = -190$, $c_2 = -190$, $d_1 = 300$ and $d_2 = 300$. In this case, noise variance is $\sigma_\epsilon = 0.5$ Results are presented in Fig. 2. Error in α estimation during the first 20 iterations is presented in Fig. 2i. Algorithm for rigid body separation is not too sensitive on accuracy of the dechirping parameter α, and quite accurate estimation is obtained after only few iterations. Results indicate that in noisy case rigid body separation from m-D is successful.

VI. Conclusion

In this paper we consider the separation of rigid body from m-D in case when target acceleration is not compensated. The unknown compensation parameter is found using a simple iterative procedure, based on the LPFT. After the signal is dechirped using the optimal compensation parameter found by the proposed algorithm, the rigid body is separated using the standard L-statistics procedure based on the STFT.

References

[1] LJ. Stanković, M. Daković, T. Thayaparan, and V. Popović-Bugarin, "Micro-Doppler Removal in the Radar Imaging Analysis" *IEEE Trans. on Aerospace and El. Sys.*, Vol. 49, No. 2, April 2013, pp.1234–1250

[2] LJ. Stanković, V. Popović-Bugarin, and F. Radenović, "Genetic algorithm for rigid body reconstruction after micro-doppler removal in the radar imaging analysis" *Sig. Process.*, Vol. 93, Jan 2013.

[3] V. C. Chen, F. Li, S. S. Ho and H. Wechsler, "Analysis of micro-Doppler signatures," *in IEE Proceedings – Radar, Sonar and Navigation*, vol. 150, no. 4, pp. 271-6-, 1 Aug. 2003.

[4] V. C. Chen, F. Li, S. S. Ho and H. Wechsler, "Micro-Doppler effect in radar: phenomenon, model, and simulation study," *in IEEE Trans. on Aerospace and El. Sys.*, vol. 42, no. 1, pp. 2-21, Jan. 2006.

[5] X. Bai, F. Zhou, M. Xing and Z. Bao, "High Resolution ISAR Imaging of Targets with Rotating Parts textquotedblright *in IEEE Transactions on Aerospace and Electronic Systems*, vol. 47, no. 4, pp. 2530-2543, Oct 2011.

[6] J. Li and H. Ling, "Application of adaptive chirplet representation for ISAR feature extraction from targets with rotating parts," *in IEE Proc. - Radar, Sonar and Navigation*, vol. 150, no. 4, pp. 284–91, 1 Aug. 2003.

[7] Y. Wang, Y.-C. Jiang, "ISAR imaging of ship target with complex motion based on new approach of parameters estimation for polynomial phase signal," *EURASIP Journal on Advances in Signal Processing* 2011(2011) ArticleID 425203, 9 pp.

[8] L. Stanković, M. Daković and T. Thayaparan, *Time–Frequency Signal Analysis with Application*, Artech House, 2013

[9] B. Boashash, *Time-Frequency Signal Analysis and Processing –A Comprehensive Reference*, Elsevier Science, Oxford, 2003.

[10] B. Boashash, "Estimating and interpreting the instantaneous frequency of a signal –Part 1: Fundamentals," *Proc. of the IEEE*, vol. 80, no.4, pp. 519–538, April 1992.

[11] LJ. Stanković, I. Orović, S. Stanković, and M. Amin, "Compressive Sensing Based Separation of Non-Stationary and Stationary Signals Overlapping in Time-Frequency," *IEEE Transactions on Signal Processing*, Vol. 61, no. 18, pp. 4562 — 4572, Sept. 2013

[12] LJ. Stanković, "A measure of some time-frequency distributions concentration," *Signal Processing*, vol. 81, pp. 621–631, Mar. 2001

[13] LJ. Stanković, D. Mandić, M. Daković, and M. Brajović, "Time-frequency decomposition of multivariate multicomponent signals," *Signal Processing*, vol. 142, pp. 468–479, January 2018